BED DRAG COEFFICIENT VARIABILITY IN A TIDAL ESTUARY: FIELD MEASUREMENTS AND NUMERICAL MODELING

By Jeremy D. BRICKER[1], Satoshi INAGAKI[2], and Stephen G. MONISMITH[3]

[1]Environmental Fluid Mechanics Laboratory, Department of Civil and Environmental Engineering, Stanford University, Stanford, CA 94305-4020, USA; now Research Associate at the Department of Civil Engineering, Kobe University, 1-1 Rokkodai-cho, Nada-ku, Kobe, 657-8501, JAPAN
email: bricker@stanfordalumni.org
[2]Senior Research Engineer, Environmental Engineering Department, Kajima Technical Research Institute, 2-19-1, Tobitakyu, Chofu-shi, Tokyo 182-0036, JAPAN
[3]Professor, Environmental Fluid Mechanics and Hydrology, Department of Civil and Environmental Engineering, Stanford University, Stanford, CA 94305-4020, USA

In this paper, we report the results of a study of the variation of shear stress and the bottom drag coefficient C_D with sea state and currents at a shallow site in San Francisco Bay. Via field experiments, we find that the model of Styles & Glenn[1], though formulated to predict C_D and shear stress under ocean swell on the continental shelf, accurately predicts enhanced drag and mean stress under wind waves in an estuary, albeit only very close to the bed. Higher up in the water column, the steady wind-driven boundary layer at the free surface overlaps with the steady bottom boundary layer, and this overlap needs to be accounted for to accurately model shear stress.

Applying the enhanced C_D of Styles & Glenn to the estuarine circulation model TRIM-3D of Gross et al[2] and Inagaki et al[3], we find that enhanced drag under wind waves retards the flushing of contaminants and sediment in South San Francisco Bay, and it enhances channel-shoal asymmetry.

Key Words: *Shear stress, drag coefficient, roughness, waves, tides, turbulence, circulation, estuary*

1. INTRODUCTION

An understanding of the bottom drag coefficient is essential for accurate modeling of hydrodynamics and sediment transport in estuaries, rivers, lakes, and on the continental shelf. The bottom drag coefficient C_D is typically defined by

$$\tau_c = \rho C_d |U| U \tag{1}$$

where τ_c is the shear stress at the bed, ρ is water density, and U is the velocity of the mean current at height z_r. C_D is nearly equivalent to the roughness length $z_0=k_b/30$ that appears in the log law

$$U = \frac{u_*}{\kappa} \ln\left(\frac{30 z_r}{k_b}\right) \tag{2}$$

where u_* is the shear velocity and $\kappa \approx 0.41$ is Von Karman's constant. The log law assumes that flow is taking place in the region of the steady bottom boundary layer (the inner or overlap layers) in which shear stress is constant ($\overline{u`w`} = u_*^2$) and eddy viscosity is increasing linearly away from the bed. Combining equation (1) with equation (2) results in

$$C_d = \left[\frac{\kappa}{\ln(30 z_r / k_b)}\right]^2 \tag{3}$$

as discussed in Gross et al[2].

In lieu of stratification, the value of C_D depends upon bed sediment grain size or bedforms. Drag is further enhanced when surface waves are long enough to reach the bed ($\lambda_{wave}/2$>depth). In this case, the thin, oscillatory wave bottom boundary layer experiences greater turbulence than the thicker, steady current bottom boundary layer (bbl). More flow momentum is leaked to the bed, resulting in a very high "apparent roughness" outside the wave bbl.

Physical roughness has been studied well in the field[4], but apparent roughness has only been measured on the continental shelf[5),6)], not in estuaries. Grant and Madsen[7] and Styles & Glenn[1] (hereafter called SG2000) provided the standard model for determining apparent roughness via theoretical means. In this model, apparent roughness is the manifestation of the wave bbl's enhanced turbulence on the region above the wave bbl. Enhanced turbulence within the wave bbl causes more momentum from the mean flow (above the wave bbl) to be transported to the bed, resulting in greater drag on the mean flow. Since circulation models used in coastal and environmental engineering do not resolve the wave bbl itself, correct prediction of apparent roughness

is necessary for these models to accurately determine mean flow over shallow regions. The theory presented in SG2000 was formulated for ocean swell propagating over the continental shelf, however, and not estuaries, where the wind-driven steady surface boundary layer overlaps with the frictional steady bottom boundary layer. The questions we set out to answer were thus:

1. *"how well does SG2000, while formulated for ocean swell over the continental shelf, predict shear stress and the bed drag coefficient under wind waves in an estuary?"*
2. *"what are the effects of variable roughness on hydrodynamics and contaminant and sediment transport in South San Francisco Bay?"*

2. EXPERIMENTS

To investigate variation of water column shear stresses and the bed drag coefficient under wind waves on the shoals of a tidal estuary, we ran experiments at Coyote Point in South San Francisco Bay (figure 1) during June of 2000 and June-July of 2002. Each experiment was run for 2 weeks to capture a full spring-neap tidal cycle. Coyote Point experiences mixed semidiurnal/diurnal tides with water depth of 1 m at low spring tide, 4 m at high spring tide, and currents up to 30 cm/s during peak flood. During the summertime, a northwesterly diurnal sea breeze of 10-15 m/s blows almost every afternoon, resulting in wind waves reaching the Point with about 2-second period, 50 cm height, and frequent spilling whitecaps.

The June-July 2002 experiment consisted of a vertical array of 3 SonTek Field Acoustic Doppler Velocimeters (ADVs, at 20 cm above the bed, 53 cmab, and 153 cmab) and a NorTek Vector Velocimeter (Vector, at 95 cmab), mounted on a mast sitting approximately 90 meters north of the beach at high water. These instruments sampled three components of velocity at 25 Hz and were cabled to shore for data acquisition and synchronization with NI LabView. A Richard Brancker Research (RBR) WG-50 capacitance wave gauge was synchronized with these velocimeters, for wave-turbulence decomposition purposes.

Additional instruments included a NorTek high-resolution Acoustic Doppler Profiler (ADP), which recorded two-minute averages of 3 components of velocity in 3 cm bins, from 15 cm above the bed to a maximum of 2 meters above the bed (though this range was reduced during times of low tide or strong waves). Time-averaged measurements of tidal stage and sea state were made with a SeaBird SBE26 absolute pressure sensor (accuracy greater than 1 mm in free surface elevation).

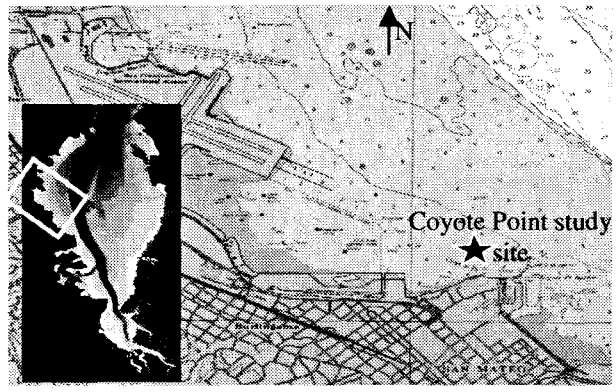

Figure 1. South San Francisco Bay and Coyote Point. Chart courtesy of NOAA Coast Survey. Chart is not to be used for navigational purposes. Inset indicates deep channel (dark shade) and shoals (light shade).

3. METHODS FOR SHEAR STRESS DETERMINATION

Using velocity time series obtained from each of the pointwise velocimeters, we calculated Reynolds stresses $\overline{u`w`}$ directly from wave-turbulence decomposed data. This wave-turbulence decomposition was carried out by the methods of Benilov & Filyushkin[8] and Shaw & Trowbridge[9], as well as the Phase Lag method described in Bricker[10]. Reynolds stresses were also calculated from spatial profiles of velocity recorded by the ADP via nonlinear least-squares fitting to a logarithmic velocity profile[10]. Knowing these Reynolds stresses, the bed drag coefficient under various conditions was then calculated from the ADP and the ADVs nearest the bed as

$$C_D = \frac{u_*^2}{U^2} \tag{4}$$

Theoretical shear stresses at the bed, as well as the bed drag coefficient, were also calculated under all conditions via SG2000. Furthermore, the theoretical stress at the height of each instrument was calculated by the assumption of a linear overlap (henceforth called the Overlap method of shear stress prediction) of bed stress from SG2000 and wind stress data from San Francisco International Airport's anemometer[10].

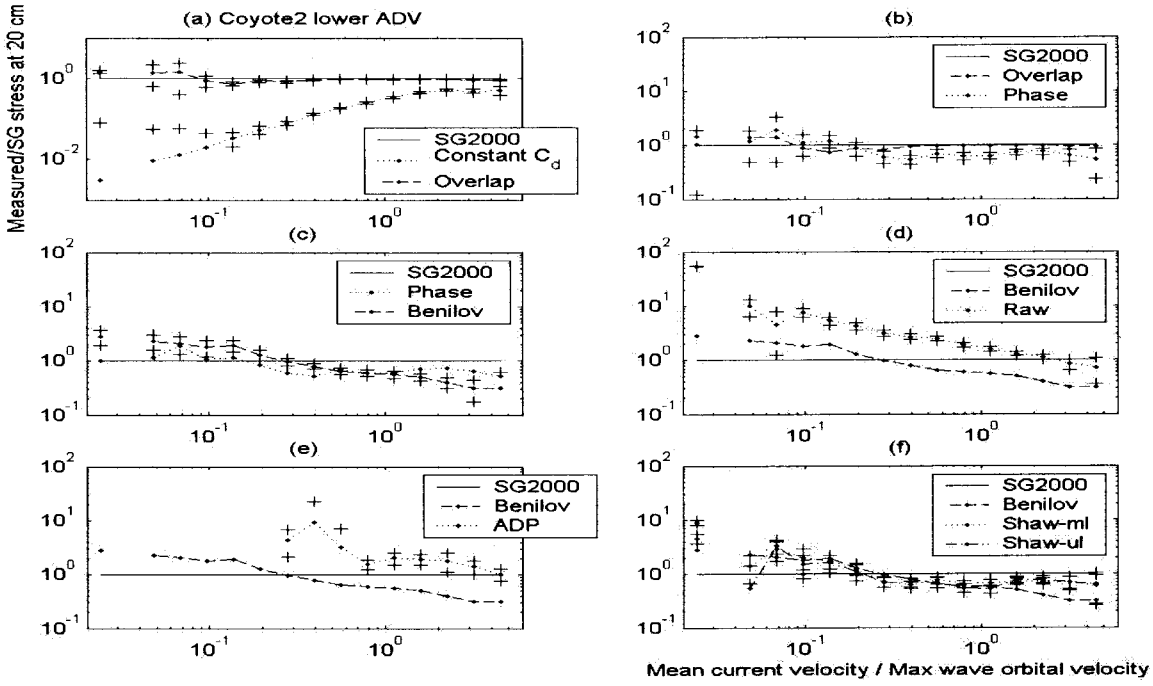

Figure 2. Ratio of shear stress obtained via various methods to shear stress obtained via SG2000 at 20 cm above the bed vs. the ratio of mean current velocity to near-bottom wave-induced orbital velocity during June-July 2002. Plusses are error bars representing 95% confidence intervals on the mean value of the stress ratio in each evenly spaced bin on the logarithmic x-axis. Error bars represent variability in stress due to variation in the independent parameters of orbital excursion and water column depth, as well as instrument error. In the figure legends, "Shaw-ml" (middle-lower) and "Shaw-ul" (upper-lower) refer to the ADV pairs used with the Shaw & Trowbridge decomposition method.

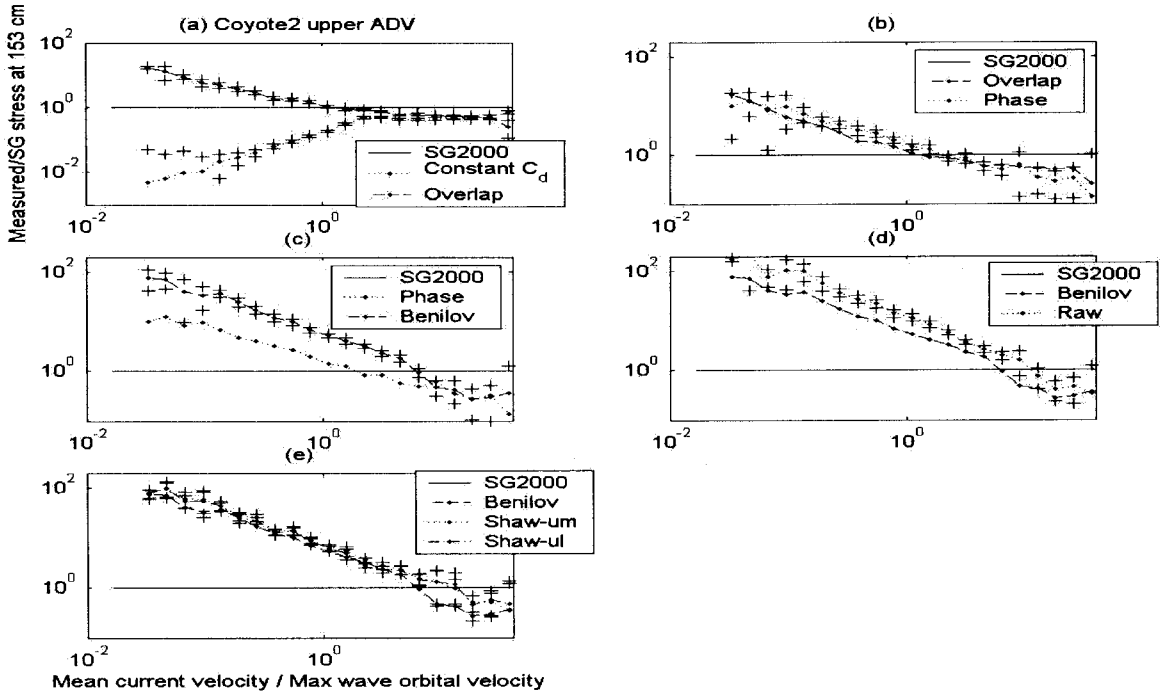

Figure 3. Same as figure 2, except uses data from the ADV at 153 cm above the bed during the June-July 2002 experiment.

4. RESULTS OF EXPERIMENTS

Effect of waves on stresses

Shear stresses computed in the ways described above are plotted in figures 2 and 3 for all conditions seen during the June-July 2002 experiment (results from the June 2000 experiment were similar). Figure 4 indicates that the drag

coefficient, calculated via equation (4) using stresses from the ADV nearest the bed, was significantly affected by waves, as Coyote Point is shallow enough for waves to "feel" the seabed. Shear stresses obtained through the ADVs, ADP, and the model of SG2000, all agree in trend. All drag coefficients converge to a value on the order of the canonical drag coefficient at 1 meter of 0.0025 in the limit where mean current velocity is much greater than the maximum near-bed wave-induced orbital velocity. All methods also reveal an increase in C_D of an order of magnitude over the canonical value when mean current velocity is 1/100 the near-bed orbital velocity.

Comparison with observations shows that SG2000 and the Overlap method predict stresses better than a constant drag coefficient does. This degree of agreement between theory and observation shows us that, despite the fact that SG2000's model was developed to predict enhanced roughness on the continental shelf under ocean swell, this model is applicable to the shallows of an estuary under the action of wind waves.

Overlap of steady surface- and bottom- boundary layers

While SG2000's predictions of stress agree with wave-turbulence decomposed near-bed (20 cm above the bed) ADV data, and with ADP data, the stress at 153 cm above the bed shows that, in the wave-dominated case, the model underestimates shear stress by up to 2 orders of magnitude. The reason for this underestimation of shear stress is the overlap of the steady wind-sheared surface boundary layer with the steady bottom boundary layer (driven by both wind and tides). During wind events, instruments high in the water column were affected by the shear stress and turbulence generated at the free surface as well as at the bed. Shear stress at these upper instruments was therefore different than it would have been had the instruments been within the bottom boundary layer only. The stress obtained via assuming an overlap of the bed and surface boundary layers, however, agrees well with wave-turbulence decomposed stress at all elevations. Wave-turbulence interaction was also observed in these experiments, and this is discussed in Bricker[10].

5. EFFECT OF ENHANCED DRAG ON CIRCULATION IN SOUTH SAN FRANCISCO BAY

We incorporated the bottom boundary layer model SG2000 into the tidal circulation model TRIM-3D[2),11)] to investigate the effect of wave-induced enhanced drag on simulation of tidal flow in South San Francisco Bay. The inputs to SG2000 are a current field and a wave field. TRIM supplied the former, while SWAN[12)] supplied the latter. The modeled current and wave fields both agreed well with data from the experiments at Coyote Point and from US Geological Survey monitoring stations throughout the Bay[10].

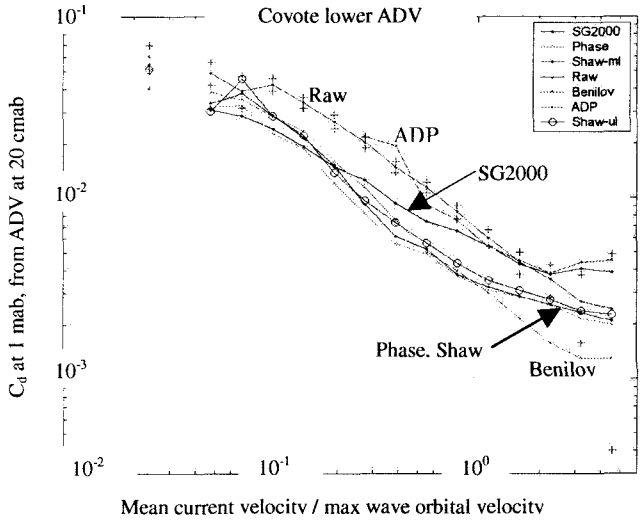

Figure 4. Drag coefficient at 1 m, as derived from the ADV 20 cm above the bed, vs. the ratio of mean current velocity to near-bottom wave-induced orbital velocity during June-July 2002

Each time step, SG2000 determined the near-bed steady current shear stress when waves were present. The drag coefficient experienced by the steady current at the following time step was then determined by equation (4), and this enhanced drag coefficicent was applied to the bottom boundary condition of TRIM-3D (equation (1)), affecting tidal circulation.

Since SG2000 predicts the increase of the drag coefficient over its calm-seas value, we still had to specity the physical roughness z_0 of the bed. We used a physical z_0 of 1.34 mm for the calm-seas roughness value throughout South Bay. This is a representative value for roughness in the channel of South Bay found by Cheng et al[4] via fitting of ADCP-derived velocity profiles to equation (2).

During calm mornings, the drag coefficient remains at its physical value throughout the entire Bay. During times of strong winds, however, it grows by more than an order of magnitude over the shoals (see figure 5). These results are similar to those observed during the Coyote Point experiments (figure 4).

Root Mean Square (rms) velocities

With uniform physical roughness only (SG2000 not used), TRIM predicted depth-averaged rms velocities in the channel to be about 50 cm/s, and over the shoals to be about 20 cm/s. Using the enhanced roughness model, rms velocities were about 2 cm/s faster in the channel and 2 cm/s slower over the shoals than those predicted by the model using uniform physical roughness.

The reason for this is the enhancement of the drag coefficient over its physical value that occurred over shoals during times of heavy seas (as in figure 5). Since the channel is too deep for waves to "feel" the seabed, however, roughness there remained at its physical value at all times. When a given pressure gradient forces seawater to flow through an area with rough shoals and a relatively smooth channel, more water flows through the channel (and less over the shoals) than occurs when roughness lengths are equal in the two regions. Since summertime winds over the Bay are diurnal, the shoals experience enhanced roughness a large portion of each day. This roughness caused the observed decrease in rms velocity over the shoals, and the increase in rms velocity in the channel. This could lead to larger cross-channel shear and thus enhanced mixing between the channel and shoals, as well as enhanced longitudinal shear-flow dispersion.

Eulerian residual velocities

TRIM predicted that tidally-averaged Eulerian residual depth-averaged velocities were generally downwind over the shoals and upwind in the channel. This is what we expect when tidal flows are averaged out, and a strong wind-driven flow dominates the residual signal.

In a simulation with variable roughness, residuals at all locations were weakened by approximately 10%. By weakening residual velocities, enhanced roughness could reduce the flushing rate of this estuary.

Passive scalar transport and flushing

To study the net effect of variable roughness on flushing, we replicated the experiment of Gross et al[2]. We released a constant 100 kg/s flow of passive scalar at the San Jose sewage treatment plant at the southern end of the Bay. As stated by Gross, "this mass was added to a cell without any volume of water, as if at each time step a constant powdered tracer mass were mixed uniformly into the... water column." The model was then run until a "dynamic steady state" was reached, in which the tidally averaged scalar field was nearly unchanging and decayed monotonically away from the source. Hydraulic residence time was calculated via the release of a passive tracer as

$$\tau_{hydraulic} = \frac{M}{\dot{M}} \qquad (5)$$

where M is the total mass in the domain, and $\dot{M}$ is the steady-state mass flow rate through the domain[2]. For the case of uniform physical roughness, the model predicted a hydraulic residence time in lower South San Francisco Bay of 18 days. With roughness from SG2000, the hydraulic residence time increased to 19 days. Signell & List[13] observed that variable roughness caused a similar decrease in flushing rates in their study of Massachusetts Bay.

Effects of variable roughness on sediment transport

Variable roughness had a significant effect on the integrated deposition minus erosion (D-E) of sediment predicted by the model. We held the unsteady component of the bed shear stress constant, while the steady component changed with the enhanced C_d of SG2000. This comparison revealed that, in the case with variable roughness, the Bay experienced more erosion (or less deposition) in the channel and more deposition (or less erosion) over the shoals than the case with uniform roughness. The magnitude of the difference averaged 10%-20% of the D-E seen by either model.

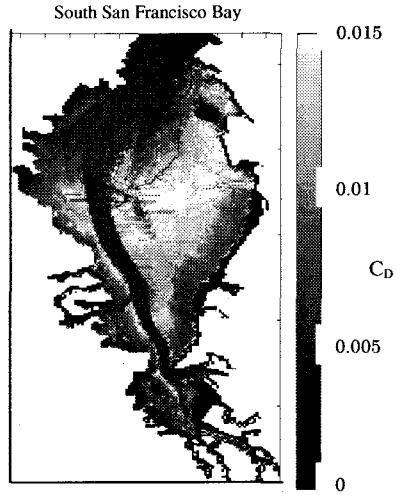

Figure 5. C_D at 1 mab determined by SG2000 using the SWAN wave model under heavy seas (westerly wind ≈ 14 m/s).

Given the effect of variable roughness on rms currents in South Bay, this difference is expected. Stronger currents in the channel lead to greater bed shear stress (equation (1)) there, which enhanced

erosion and inhibited deposition. Deposition in the channel was further reduced by the reduced transport in of sediments from the shoals, due to the retarded currents there. Over the shoals, however, reduced transport due to reduced currents acted to retain sediments close to the location at which they were first scoured from the bed. Transport of wind-wave-scoured sediments from the shoals to the channel by the ebb tide was thus inhibited, resulting in enhanced deposition on the shoals.

6. CONCLUSIONS

"How well does SG2000, while formulated for ocean swell over the continental shelf, predict shear stress and the bed drag coefficient under wind waves in an estuary?"

The enhanced steady shear stresses and drag coefficients predicted by SG2000's model agreed well with near-bottom (20 cm high) observations of C_D in the steady bottom boundary layer under wind waves on shoals. Further up in the water column, it was necessary to calculate the shear stress at both the bed (via SG2000) and the surface, and then to assume a linear variation between these two throughout the water column.

"What are the effects of variable roughness on hydrodynamics and contaminant and sediment transport in South San Francisco Bay?"

Hydrodynamic modeling results showed that the variable bed drag coefficient predicted by SG2000 had an effect on flushing and sediment transport in San Francisco Bay, especially because it is a channel-shoal system. Since the drag coefficient under heavy seas took a larger value over shoals only, tidally averaged rms velocities were enhanced in the channel and reduced over shoals. This resulted in more scouring (~10%) of sediments from the channel, and more deposition over the shoals. Since enhanced drag retarded currents over the shoals when wave-induced erosion was largest, transport of sediments from the shoals to the channel was also reduced, further enhancing depositional tendencies over the shoals, and reducing deposition in the channel.

By releasing a passive tracer from the San Jose POTW at a constant rate, we determined that variable roughness has the net effect of reducing the flushing rate in South San Francisco Bay. The hydraulic residence time in lower South San Francisco Bay increased from 18 days to 19 days when variable roughness was accounted for.

ACKNOWLEDGEMENT: Funding for this work was provided by the UPS foundation and by the Office of Naval Research.

REFERENCES

1) Styles, R., and Glenn, S. M. Modeling stratified wave and current bottom boundary layers on the continental shelf. *Journal of Geophysical Research.* v 105 n C10 pp 24119-24139. 2000.
2) Gross, E. S., Koseff, J. R., and Monismith, S. G. Three-dimensional salinity simulations of south San Francisco Bay. *ASCE Journal of Hydraulic Engineering.* v 125 n 11 pp 1199-1209. 1999.
3) Inagaki, S., Monismith, S.G. Koseff, J.R., and Bricker, J.D. Sediment transport simulation in South San Francisco Bay. Proceedings of Coastal Engineering, JSCE, v48, pp641-645, 2001.
4) Cheng, R. T., Ling C. H., and Gartner J. G. Estimates of bottom roughness length and bottom shear stress in South San Francisco Bay, California. *Journal of Geophysical Research.* v 104 n C4 pp 7715-7728. 1999.
5) Cacchione, D. A., Drake, D. E., Ferreira, J. T., and Tate, G. B. Bottom stress estimates and sand transport on northern California inner continental shelf. *Continental Shelf Research.* V14 n10/11 pp1273-1289. 1994.
6) Green, M., and McCave. Seabed drag coefficient under tidal currents in the eastern Irish Sea. *Journal of Geophysical Research.* v100 nC8 pp16057-16069. 1995.
7) Grant, W. D., and Madsen, O. S. Combined Wave and Current Interaction with a Rough Bottom. *Journal of Geophysical Research.* v84 nC4 pp1797-1808. 1979.
8) Benilov, A. Y. and Filyushkin, B. N. Application of methods of linear filtration to an analysis of fluctuations in the surface layer of the sea. *Izvestiya Atmospheric and Oceanic Physics.* v6 n8 pp810-819. 1970.
9) Shaw, W. J., and Trowbridge, J. H. The Direct Estimation of Near-bottom Turbulent Fluxes in the Presence of Energetic Wave Motions. *Journal of Atmospheric and Oceanic Technology.* v 18 pp 1540-1557. 2001.
10) Bricker, J. D. Bed drag coefficient variability under wind waves in a tidal estuary: field measurements and numerical modeling. Stanford University Ph.D. thesis. 2003.
11) Casulli, V., and Cattani, E. Stability, accuracy, and efficiency of a semi-implicit method for three-dimensional shallow water flow. *Computers and Mathematics with Applications.* v 27 n 4 pp 99-112. 1994.
12) Booij, N., Ris, R. C., and Holthuijsen, L. H. A third-generation wave model for coastal regions 1. Model description and validation. *Journal of Geophysical Research.* v104 nC4 pp7649-7666. 1999.
13) Signell, R. P., and List, J. H. Effect of wave-enhanced bottom friction on storm-driven circulation in Massachusetts Bay. *Journal of Waterway, Port, Coastal, and Ocean Engineering.* v123 n5 pp233-239. 1997

(Received September 30, 2003)